Postprint of: Cichowska-Kopczyńska I., Mioduska J., Karczewski J., Double ZIF-L structures with exceptional CO_2 capacity, CHEMICAL ENGINEERING RESEARCH & DESIGN, Vol. 188 (2022), pp. 1077-1082, DOI: 10.1016/j.cherd.2022.11.004

Double ZIF-L structures with exceptional CO_2 capacity

IWONA CICHOWSKA-KOPCZYNSKA[a*], JOANNA MIODUSKA[a], JAKUB KARCZEWSKI[b]

Gdańsk University of Technology, Narutowicza 11/12 Str., Gdańsk, Poland

[a] Department of Process Engineering and Chemical Technology, Faculty of Chemistry,
[b] Institute of Nanotechnology and Materials Engineering, Faculty of Applied Physics and Mathematics

[*]Corresponding author: iwona.kopczynska@pg.edu.pl
Phone: +48 58 347 18 69
Fax: +48 58 347 20 65

Abstract

Carbon dioxide emission is an emerging problem nowadays and new methods are designed for its control. In this article, a report on the formation of zeolitic imidazole framework with an apparent double leaf-like morphology DZIF-L is given. The special structure of the materials prevents from aggregation of the particles providing remarkable CO_2 capacity. At 0.1 MPa the CO_2 uptake was 2.99 ± 0.06 mmol/g. The capacity of synthesized material is higher than that of any other structure that was so far identified between single ZIF-L and ZIF-8. Fourier transform infrared (FT-IR), X-ray diffraction (XRD), scanning electron microscopy (SEM) and Brunauer-Emmett-Teller surface area analysis were used to characterize the material.

Key words: zeolitic imidazole framework, carbon dioxide, uptake, adsorption

1. Introduction

The rapid increase of the population and resulting energy consumption contribute to a high emission of pollutants to the atmosphere, from which carbon dioxide is an emerging problem. Therefore, there is a great necessity to develop new effective separation technologies. In recent decades a lot of focus was put on new solvents like ionic liquids or deep eutectic solvents and their use in membrane separation process as well as mixed matrix membranes filled with metal organic frameworks (MOFs). Mixed matrix membranes can incorporate several types of fillers, like zeolites [1–3], silica, activated carbon [4], carbon molecular sieves [5,6], metal organic frameworks (MOFs) [7] and other. Metal-organic frameworks are crystalline materials with high surface area and porosity that form a network of metal ion node coordinated to organic ligands. They are obtained in the reaction of metal salts and organic linkers, like imidazolates, carboxylates etc. which have oxygen or nitrogen atoms built in. Typically, MOFs are obtained by solvothermal method, where the organic and metal precursors are dissolved in polar solvents like water or alcohol [8] and simply mixed to make the product that precipitates from the solution.

Among MOFs there is a large group of materials based on Zn or Co that together with imidazole ligand constitute large molecular structures called zeolitic imidazole frameworks (ZIFs). The bond angle in ZIFs is similar to that in zeolites therefore ZIFs present many characteristics specific for zeolites like stability, high surface area and crystallinity [9] and at the same time advantages of MOFs. Unlike some MOFs ZIFs can be obtained easier and cheaper and are stable in moist conditions and at high temperatures. ZIFs has been widely studied due to the simplicity of the synthesis procedure, sorption capacity and potential in use as a filler for gas separation membranes.

Even though the preparation procedure seems to be simple, it should be carefully developed, because concentration of chemicals, solvent type, pH, agitation speed, temperature, additives [10], aging etc. can have a remarkable effect on the ZIF type, its structure, shape and size. Mainly ZIF-8 is studied in the literature, but lately two-dimensional leaf-like shape ZIF-L gained attention. There are several types of ZIF-L reported in the literature, flower-like, hierarchical and single cushion-shape ZIF-L, which is the most frequently examined [11–13].

Single ZIF-L are mostly studied in the membrane systems. One of the examples is H_2/CO_2 separation examined by Yang et al. The authors obtained selectivity of ~208 [14]. Pebax membranes incorporating ZIF-L for CO_2/CH_4 separation with the selectivity reaching 19 were also used [15]. Low et al. used ZIF-L nanoflakes in polyethersulfone ultrafiltration membrane [11].Valencia et al. used leaf-like zeolite imidazole framework foams for carbon dioxide capture with the capacity of 0.75 mmol/g for 50% ZIF-L in the foam, for pure powder CO_2 capacity was 0.9 mmol/g at 298 K and 1 bar [16]. Similar results for carbon dioxide capacity of single ZIF-L were obtained by Chen et al. [17]. The authors proved higher CO_2 capacity of ZIF-L (0.94 mmol/g) than that of ZIF-8 (0.68 mmol/g), ZIF-95 and ZIF-100.

In the literature more complex forms of ZIF-L can also be found, these are flower-shaped and hierarchical shapes. Synthesis of flower shaped ZIF-L was reported by Wang et al [18]. CO_2 capacity of hierarchical ZIF-L was determined by Ding et al at the level of 1.56 mmol/g. Park et al examined wide range of different ZIFs and reported that ZIF-8 can be obtained by crystal transformation of ZIF-L [19]. Moreover, in research focused on single ZIF-L, a propeller-shaped double structures occur as a defect. In some studies the CO_2 uptake of single ZIF-L occurred to be higher than that of ZIF-8 [17] and lower than that of hierarchical and flower-shaped ZIF-L [18,20], for that reason this research focused on obtaining the least complex three-dimensional ZIF-L structure, namely double ZIF-L (DZIF-L). This structure should limit aggregation in comparison to single ZIF-L and ZIF-8 that tend to agglomerate forming a dense layer. Since ZIF-L are often dedicated to membrane systems, such behaviour would decrease the permeability of resulting membrane and double ZIF-L could resist from aggregation and may be capable of forming oriented porous surface. In this regard, we expect that this special double leaf like shape has potential in gas separation applications.

2. Experimental

2.1. Preparation of DZIF-L

Hydrothermal method for DZIF-L fabrication was used. The molar ratio of the components was set at 1:8:2250, accordingly for Zn^{2+}:Im:H_2O. Zn^{2+} ions originated from $Zn(NO_3)_2 \cdot 6H_2O$, supplied by Chempur Poland, Im source was 2-methylimidazole (99%) from Acros Organics and methanol (99.8%) from Avantor Performance Materials Poland S.A. All chemicals were used without further purification. The water solutions of the components were prepared at 298 K and mixed together for the reaction. The reaction mixture was stirred with a speed of 500 rpm for 5 hours at 288 K. The resulting precipitate was then twice washed with deionised water and twice with methanol, each time being collected by centrifugation (4000 rpm for 10 minutes). Then the sample was dried in a vacuum oven at 343 K overnight.

2.2. Characterization

Prior to the measurements samples were degassed under vacuum at 423 K for 24 h. Nitrogen adsorption isotherms and total pore volumes were measured using Micromeritics Gemini V Analyzer at 77 K. Nitrogen adsorption curves were determined in the range of P/P_0 from 0.01 to 0.98. Specific surface area was calculated using the Brunauer–Emmett–Teller (BET) linear equation in the approximate relative pressure range from P/P_0 0.05 to 0.3. Total pore volume was calculated at P/P_0 0.95.

The morphology of the samples with particle size analysis was investigated by the Schottky field emission scanning electron microscope SEM (FEI Quanta FEG 250) with an ET secondary electron detector. The beam acceleration voltage was kept at 10 kV. The samples were coated with gold before imaging.

X-ray diffraction measurements were made using Cu-Kα radiation on a Rigaku Miniflex 600. XRD data was obtained within the angle range of 5-50 degrees operating at a scanning rate of 1° min^{-1}.

The Fourier transform infrared spectrum was recorded in transmittance mode with x cm^{-1} spectra cl resolution using ThermoSCIENTIFIC Nicolet iS10.

The CO_2 adsorption capacity was determined using volumetric method as described in the literature [18,20]. Briefly, the capacity was determined at 298 K up to 250 kPa. Prior to the test, dry and degassed samples were placed in the testing chamber and kept under vacuum for 12 h at 373 K. The samples were cooled to 298 K and pure CO_2 was introduced to reach equilibrium. The equilibrium pressure was recorded when the value did not change over 4 hours.

3. Results and discussion

The sample morphology was characterized by SEM. The material is white and is a 3D framework with well-defined leaf-shaped crystals, composed of two ZIF-L structures crossing each other along the long or short axis. The morphology is well defined and different from that of single ZIF-L and flower-shaped ZIL-L. As shown in Figure 1 the average nominal size of the DZIF-L was found to be 7.8 μm along the long axis and 3.4 μm along the short axis. The main difference between these two identified structures is the ration of length to width

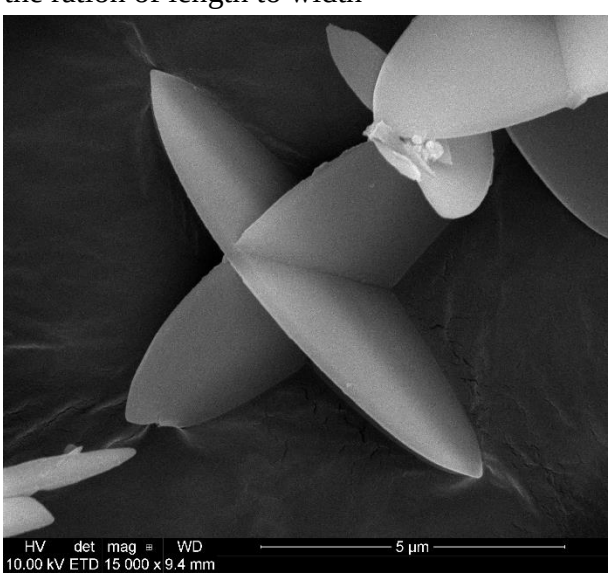

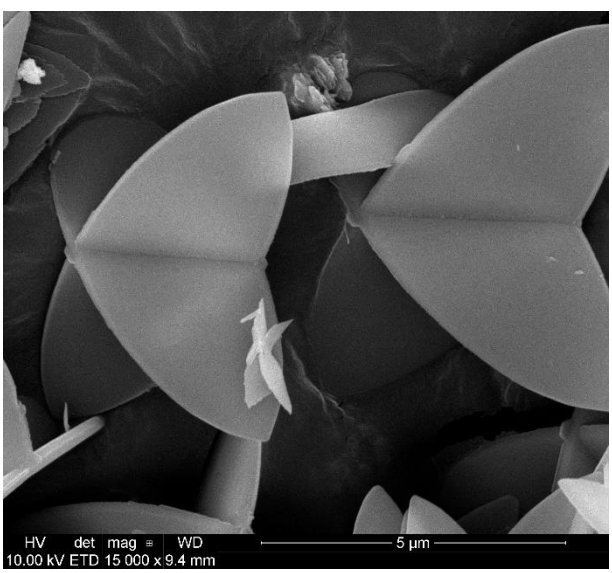

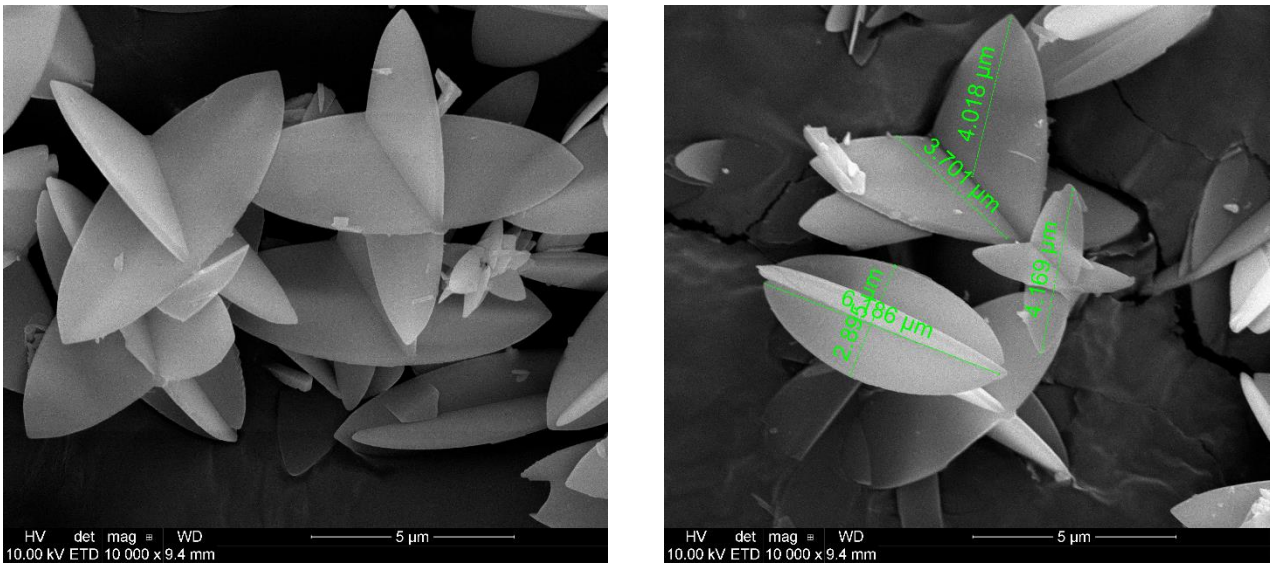

Figure 1 SEM micrograph of the DZIF-L

The structure of obtained material was analysed using XRD as shown in Figure 2 a). All the diffraction peak positions agree well with the spectra reported in the literature for ZIF-L with relatively strongest XRD peaks observed at 2θ of 11.1º, 15.3º, 17.2º, 18.1º, 29.2º that stay in agreement with the several reports from ZIF-L studies [21,22].

a)

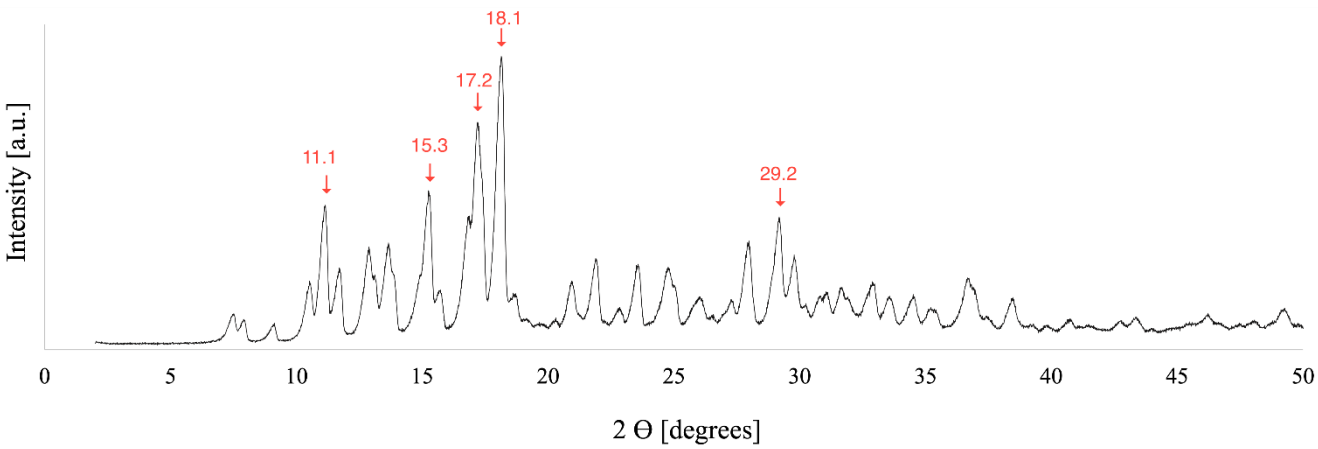

b)

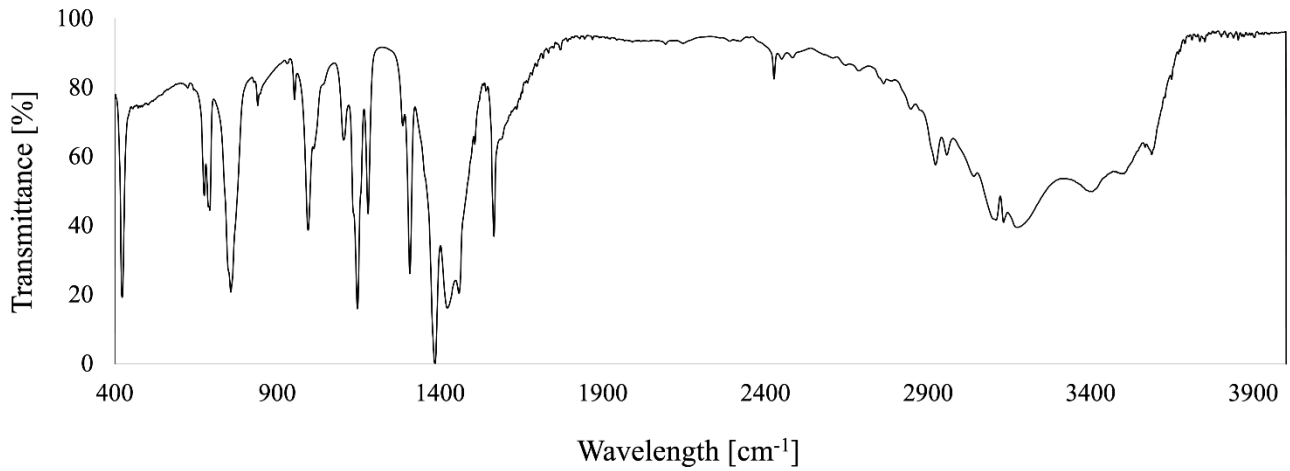

Figure 2 a) XRD pattern and b) FTIR spectrum of DZIF-L

As shown in Figure 2 b) the chemical structure of the DZIF-L was verified by FTIR spectroscopy. Presence of the characteristic peaks for C=N, C-N, CH, and Zn-N was confirmed and agrees well with ones reported in the literature for ZIF-L.

The results indicated the main bands at 422 cm^{-1}, 692 cm^{-1}, 758 cm^{-1}, 995 cm^{-1}, 1147 cm^{-1}, 1179 cm^{-1}, 1307 cm^{-1}, 1386 cm^{-1}, 1566 cm^{-1} and 2426 cm^{-1}. The absorption band at 422 cm^{-1} represents stretching of Zn-N. The bands in the spectral region of 600-800 cm-1 are associated with bending of the imidazole ring outside the plane, those in 900-1350 region with in-plane bending. Peaks at 1307 cm^{-1}, 1179 cm^{-1}, 1147cm^{-1} and 995 cm^{-1} are associated with C-N stretching vibrations. Peaks at 1386 cm^{-1} and 758 cm^{-1} can be assigned to CH aromatic bending. The C=N bonds are represented by peak at about 1566 cm^{-1} and are attributed to stretching vibration. The peak at about 2426 cm-1 is ascribed to N-H···N hydrogen bond, while the broad band from 2350 to 3700 N-H···N results from the bridging the ZIF-L layers and the N-H group in methylimidazole [19].

For the obtained DZIF-L, N_2 adsorption measurement was performed to determine the specific surface area, as presented in Figure 4. The isotherm is of type II according to the IUPAC classification, which indicates the macroporous structure of the material.

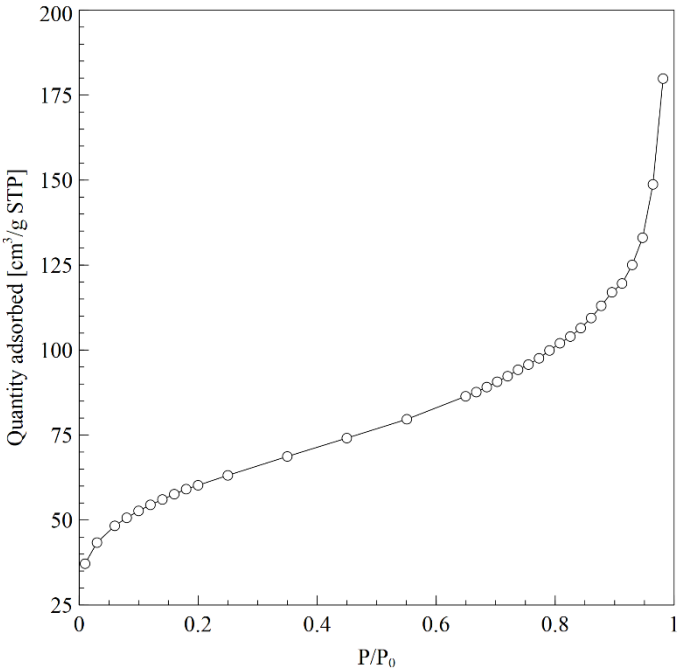

Figure 3 Exemplary N_2 adsorption isotherm of the DZIF-L

The specific surface area of the obtained DZIF-L samples was 223 ± 10 m^2/g and is in a good agreement with the values presented in the literature for individual ZIF-L structures. The area is larger than that observed for leaf-like ZIF-L and lower than that reported for flower-shaped structures and ZIF-8. For single ZIF-L, Chen et al. reported 161 m^2/g and micropore volume of 0.066 cm^3/g [17], by Deacon et al. reported 93 m^2/g for single ZIF-L and 1651 for ZIF-8 [23]. Hierarchical structures were proved to have 304 m^2/g [20]. Still, values reported by different authors vary. Low et al. obtained 18 m^2/g and porosity of 0.02 cm^3/g for single ZIF-L [19]. Kahn et al. obtained surface area of 2.5 m^2/g and pore volume of 0.0034 cm^3/g for 2D ZIF-L and 1472 m^2/g and 0.6067 cm^3/g for ZIF-8 [24].

Within this study, for DZIF-L we obtained total pore volume of 0.188 ± 0.02 cm^3/g at P/P_0 of 0.95, which is compliant with the values reported by other researchers, higher than the values obtained for single ZIF-L and lower than the values reported for ZIF-8.

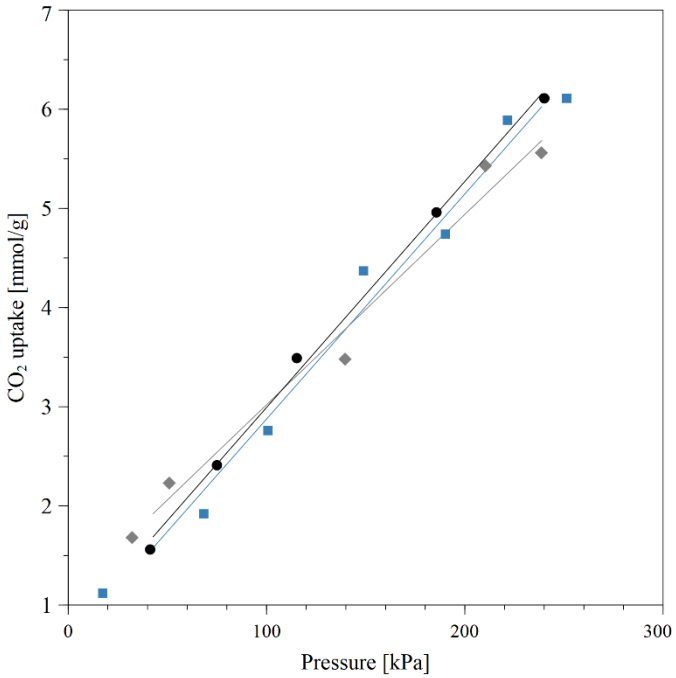

Figure 4 Adsorption isotherm of CO_2 by DZIF-L at 298 K (● ; ■ ; ◆ represent experimental points of three experiments)

The adsorption isotherms of CO_2 by the DZIF-L are shown in Figure 4. In the three experiments at 0.1 MPa the CO_2 uptake was 3.02, 3.05 and 2.91 mmol/g, resulting in the average capacity of 2.99 ± 0.06 mmol/g. The capacity of synthesized material is higher than that of any other structure that was so far identified between single ZIF-L and ZIF-8 (Figure 5).

Only Shi et al. obtained comparable capacity of ZIF-8. The authors performed test on CO_2 adsorption capacity of ZIF-8 obtained at different conditions and reported capacity in a range 2.18 – 3.04 g/mmol. The structure of 3.04 mml/g capacity was synthesized at 358 K [25]. Flower-shaped ZIF-L synthesized by Wang et al. exhibited CO_2 uptake of 1.15 mmol/g at 298 K and 0.1 MPa [18]. Chen et al. reported 0.94 mmol/g uptake for single ZIF-L and 0.68 mmol/g for ZIF-8 [17]. Hierarchical ZIF-L structures, which is between flower-shaped ZIF and double- ZIF-L, obtained by Ding et al. exhibited 1.56 mmol/g uptake with 304 m^2/g of surface area [20]. Double ZIF-L presents higher CO_2 capacity than single one. This is attributed to the structure, and anti-aggregation properties [18]. The special structure of the particles prevents from stacking together as it is seen in case of leaf-like ZIF. Moreover ZIF-L has a smaller pore size and higher density of metal atoms per unit volume than ZIF-8 [17] and despite the larger surface area of ZIF-8, double ZIF-L has a comparable CO_2 adsorption capacity because of the special shape and cavity. It enables a strong interaction between CO_2 and the 2-methylimidazole originating from the short distance of O atom in CO_2 and H atoms in methylimidazole [17].

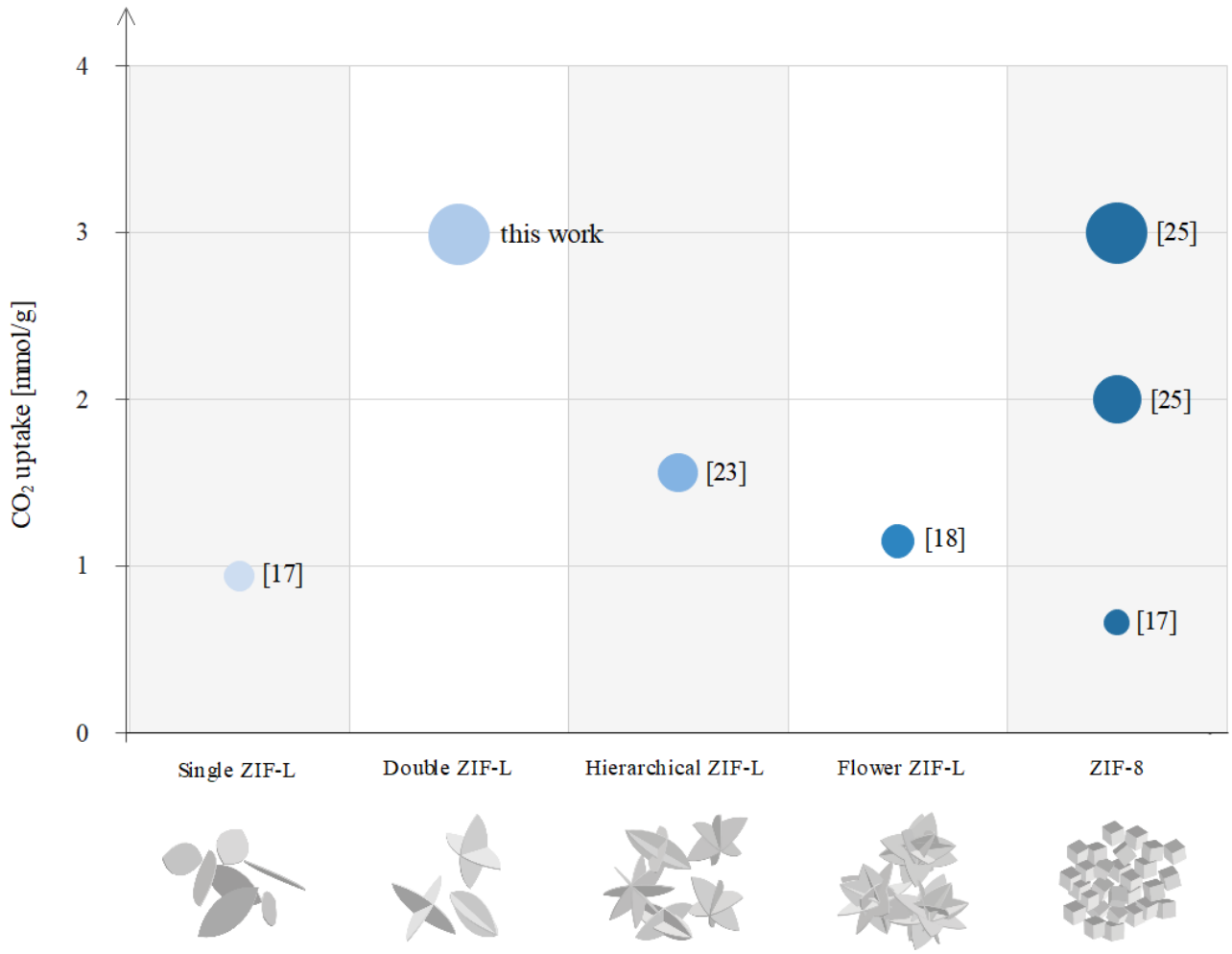

Figure 5 CO_2 uptake of individual ZIF-L structures

4. Conclusions

To our best knowledge it is the first time when the apparent DZIF-L structure was obtained for CO_2 capture. Literature data show that on the transition route from ZIF-L to ZIF-8 there also three other structures that can be distinguished, namely flower-shaped ZIF-L, hierarchical ZIF-L and double ZIF-L obtained within this study. There is only one report in which the authors described ZIF-8 with CO_2 capacity at the same level [25] as capacity of DZIF-L obtained in this research. In general, the specific surface area increases as the ZIF-L transforms to the ZIF-8, but CO_2 capacity is higher for ZIF-L than for ZIF-8 and the intermediate structures present even higher capacity than both ZIF-L and ZIF-8. From all the structures that can be distinguished DZIF-L presented the best performance. Agglomeration can be the reason for lower capacity of single ZIF-L and ZIF-8 as the molecules stick to each other forming a dense layer that limits adsorption capacity. Within the study we succeeded in obtaining the least complex three-dimensional ZIF-L structure, that reduces aggregation and thus enables high adsorption. Since ZIF-Ls are often dedicated to membrane systems, such structure may be capable of forming oriented porous surface which can enhance permeability of resulting membrane. In this regard, we expect that the obtained double ZIF-L structure, which was proven to have remarkable CO_2 capacity in

comparison to ZIF-8, hierarchical, flower-shaped and single ZIF-L, has the potential in gas separation applications.

Declaration of Competing Interest

The authors declare that they have no known competing financial interests or personal relationships that could have appeared to influence the work reported in this paper.

Acknowledgements

This work was supported by the Faculty of Chemistry, Gdańsk University of Technology within the mini-grant project no. 034568.

Author contributions

Iwona Cichowska-Kopczyńska conceived and supervised the project, planned the experiments, performed the sorption experiments, contributed to the data analysis, interpretation and wrote the paper. Joanna Mioduska synthesized the material, performed analyses including BET analyses, FTIR, XRD, contributed to the data analysis, interpretation and paper writing. Jakub Karczewski performed the analyses.

References

[1] T.W. Pechar, S. Kim, B. Vaughan, E. Marand, M. Tsapatsis, H.K. Jeong, C.J. Cornelius, Fabrication and characterization of polyimide-zeolite L mixed matrix membranes for gas separations, J. Memb. Sci. 277 (2006) 195–202. https://doi.org/10.1016/j.memsci.2005.10.029.

[2] M.G. Süer, N. Baç, L. Yilmaz, Gas permeation characteristics of polymer-zeolite mixed matrix membranes, J. Memb. Sci. 91 (1994) 77–86. https://doi.org/10.1016/0376-7388(94)00018-2.

[3] B. Ozturk, F. Demirciyeva, Comparison of biogas upgrading performances of different mixed matrix membranes, Chem. Eng. J. 222 (2013) 209–217. https://doi.org/10.1016/j.cej.2013.02.062.

[4] M. Anson, J. Marchese, E. Garis, N. Ochoa, C. Pagliero, ABS copolymer-activated carbon mixed matrix membranes for CO 2/CH4 separation, J. Memb. Sci. 243 (2004) 19–28. https://doi.org/10.1016/j.memsci.2004.05.008.

[5] R. Mahajan, W.J. Koros, Separation Materials, Ind. Eng. Chem. Res. 39 (2000) 2692–2696.

[6] D.Q. Vu, W.J. Koros, S.J. Miller, Mixed matrix membranes using carbon molecular sieves: I. Preparation and experimental results, J. Memb. Sci. 211 (2003) 311–334. https://doi.org/10.1016/S0376-7388(02)00429-5.

[7] M. Arjmandi, M. Pakizeh, Mixed matrix membranes incorporated with cubic-MOF-5 for improved polyetherimide gas separation membranes: Theory and experiment, J. Ind. Eng. Chem. 20 (2014) 3857–3868. https://doi.org/10.1016/j.jiec.2013.12.091.

[8] J.L.C. Rowsell, O.M. Yaghi, Metal-organic frameworks: A new class of porous materials, Microporous Mesoporous Mater. 73 (2004) 3–14. https://doi.org/10.1016/j.micromeso.2004.03.034.

[9] M.S. Mirqasemi, M. Homayoonfal, M. Rezakazemi, Zeolitic imidazolate framework membranes for gas and water purification, Springer International Publishing, 2020. https://doi.org/10.1007/s10311-019-00933-6.

[10] J. Cravillon, R. Nayuk, S. Springer, A. Feldhoff, K. Huber, M. Wiebcke, Controlling Zeolitic Imidazolate Framework Nano- and Microcrystal Formation: Insight into Crystal Growth by

Time-Resolved In Situ Static Light Scattering, Chem. Mater. 23 (2011) 2130–2141. https://doi.org/10.1021/cm103571y.
[11] Z.X. Low, A. Razmjou, K. Wang, S. Gray, M. Duke, H. Wang, Effect of addition of two-dimensional ZIF-L nanoflakes on the properties of polyethersulfone ultrafiltration membrane, J. Memb. Sci. 460 (2014) 9–17. https://doi.org/10.1016/j.memsci.2014.02.026.
[12] C. Zhang, J. Yan, T. Ji, D. Du, Y. Sun, L. Liu, X. Zhang, Y. Liu, Fabrication of highly (110)-Oriented ZIF-8 membrane at low temperature using nanosheet seed layer, J. Memb. Sci. 641 (2022) 119915. https://doi.org/10.1016/j.memsci.2021.119915.
[13] Z. Zhong, J. Yao, R. Chen, Z. Low, M. He, J.Z. Liu, H. Wang, Oriented two-dimensional zeolitic imidazolate framework-L membranes and their gas permeation properties, J. Mater. Chem. A. 3 (2015) 15715–15722. https://doi.org/10.1039/c5ta03707g.
[14] K. Yang, S. Hu, Y. Ban, Y. Zhou, N. Cao, M. Zhao, Y. Xiao, W. Li, W. Yang, ZIF-L membrane with a membrane-interlocked-support composite architecture for H2/CO2 separation, Sci. Bull. 66 (2021) 1869–1876. https://doi.org/10.1016/j.scib.2021.05.006.
[15] W. Zhu, X. Li, Y. Sun, R. Guo, S. Ding, Introducing hydrophilic ultra-thin ZIF-L into mixed matrix membranes for CO2/CH4 separation, RSC Adv. 9 (2019) 23390–23399. https://doi.org/10.1039/c9ra04147h.
[16] L. Valencia, H.N. Abdelhamid, Nanocellulose leaf-like zeolitic imidazolate framework (ZIF-L) foams for selective capture of carbon dioxide, Carbohydr. Polym. 213 (2019) 338–345. https://doi.org/10.1016/j.carbpol.2019.03.011.
[17] R. Chen, J. Yao, Q. Gu, S. Smeets, C. Baerlocher, H. Gu, D. Zhu, W. Morris, O.M. Yaghi, H. Wang, A two-dimensional zeolitic imidazolate framework with a cushion-shaped cavity for CO2 adsorption, Chem. Commun. 49 (2013) 9500–9502. https://doi.org/10.1039/c3cc44342f.
[18] S. Wang, B. Zang, Y. Chang, H. Chen, Synthesis and carbon dioxide capture properties of flower-shaped zeolitic imidazolate framework-L, CrystEngComm. 21 (2019) 6536–6544. https://doi.org/10.1039/c9ce00833k.
[19] Z.X. Low, J. Yao, Q. Liu, M. He, Z. Wang, A.K. Suresh, J. Bellare, H. Wang, Crystal transformation in zeolitic-imidazolate framework, Cryst. Growth Des. 14 (2014) 6589–6598. https://doi.org/10.1021/cg501502r.
[20] B. Ding, X. Wang, Y. Xu, S. Feng, Y. Ding, Y. Pan, W. Xu, H. Wang, Hydrothermal preparation of hierarchical ZIF-L nanostructures for enhanced CO2 capture, J. Colloid Interface Sci. 519 (2018) 38–43. https://doi.org/10.1016/j.jcis.2018.02.047.
[21] C.J. Wijaya, S. Ismadji, H.W. Aparamarta, S. Gunawan, Facile and green synthesis of starfruit-like ZIF-L, and its optimization study, Molecules. 26 (2021). https://doi.org/10.3390/molecules26154416.
[22] C. Huang, H. Zhang, K. Zheng, Z. Zhang, Q. Jiang, J. Li, Two-dimensional hydrophilic ZIF-L as a highly-selective adsorbent for rapid phosphate removal from wastewater, Sci. Total Environ. 785 (2021). https://doi.org/10.1016/j.scitotenv.2021.147382.
[23] A. Deacon, L. Briquet, M. Malankowska, F. Massingberd-Mundy, S. Rudić, T. l. Hyde, H. Cavaye, J. Coronas, S. Poulston, T. Johnson, Understanding the ZIF-L to ZIF-8 transformation from fundamentals to fully costed kilogram-scale production, Commun. Chem. 5 (2022) 1–10. https://doi.org/10.1038/s42004-021-00613-z.
[24] I.U. Khan, M.H.D. Othman, A.F. Ismail, N. Ismail, J. Jaafar, H. Hashim, M.A. Rahman, A. Jilani, Structural transition from two-dimensional ZIF-L to three-dimensional ZIF-8 nanoparticles in aqueous room temperature synthesis with improved CO2 adsorption, Mater. Charact. 136 (2018) 407–416. https://doi.org/10.1016/j.matchar.2018.01.003.
[25] Z. Shi, Y. Yu, C. Fu, L. Wang, X. Li, Water-based synthesis of zeolitic imidazolate framework-8 for CO2 capture, RSC Adv. 7 (2017) 29227–29232. https://doi.org/10.1039/c7ra04875k.